

# Hydration-Induced Deformation of Lipid Aggregates before and after Polymerization

H. Binder,<sup>\*,†</sup> U. Dietrich,<sup>†</sup> M. Schalke,<sup>†</sup> and H. Pfeiffer<sup>‡</sup>

*Institut für Experimentelle Physik I, Universität Leipzig, Linnèstrasse 5, D-4103 Leipzig, Germany, and Department of Chemistry, Katholieke Universiteit Leuven, Celestijnenlaan 200D, 3001 Leuven, Belgium*

*Received January 19, 1999. In Final Form: April 7, 1999*

The dimensions of multibilayer stacks of lipids with terminal diene groups were studied before and after polymerization at variable hydration by means of X-ray diffraction, gravimetry, and infrared spectroscopy. The short-range hydration force acting between the bilayers of lipids with phosphatidylcholine and -ethanolamine headgroups is not affected by lipid polymerization. Consequently, contributions to the interbilayer repulsion which are caused by the mobility of individual molecules are obviously negligible at distances of less than a few tenths of nanometers. The polymerized lamellae become essentially incompressible in the direction parallel to the membrane surface owing to intermolecular covalent bonds. The infrared frequencies of the methylene stretching bands of the lipids correlate linearly with the area per molecules within the membrane plane. Consequently, infrared spectroscopy in combination with the osmotic stress technique represents a convenient method to estimate lateral compressibility qualitatively. The terminal diene groups of bis(tetradecadienoyl)phosphorylethanolamine give rise to a relatively strong component of the lateral pressure which tends to bend the lipid monolayers into inverse structures such as the H<sub>II</sub> phase.

## 1. Introduction

Lipids typically form multibilayer stacks in a humid atmosphere. Several aspects of the physicochemistry of lipids have been successfully studied on fully hydrated multilamellar ensembles such as lipid phase behavior, lipid–protein interactions, or the influence of additives on lipid structure.<sup>1</sup> When a fully hydrated multilayer array is brought to thermodynamic equilibrium with a vapor phase of reduced relative humidity, RH < 100%, the lipids dehydrate; i.e., the water is removed from the polar region of the lipids and from the interbilayer space. As a result, the polar surfaces of opposite bilayers approach each other and the lipid layers are compressed laterally, i.e., in the direction parallel to the membranes.<sup>2</sup> Moreover, the removal of water from the lipid headgroups usually causes a bending torque within each of the monolayers of the membrane. Dehydration-induced lateral compression and curvature strain are known to induce fluid/solid and lamellar/nonlamellar phase transformations in numerous lipid systems.<sup>3–6</sup>

The hydration-dependent deformation of multibilayer assemblies is well established as a standard method in lipid research.<sup>7,8</sup> This so-called osmotic stress technique

brought considerable progress in the experimental study of hydration phenomena such as the repulsive forces acting between membranes.<sup>9</sup> Some aspects of this “hydration” force remain, however, unresolved yet. For example, short-range out-of-plane fluctuations of individual lipid molecules are assumed to give a significant contribution to interbilayer repulsion on the one hand,<sup>10,11</sup> but in the sum of several arguments such molecular protrusions are suggested to be an implausible cause of hydration forces on the other hand.<sup>12</sup> The main reason that this controversy still exists is the ambiguity and/or the deficiency of experimental data about the degree of correlation between the mobility of the molecules and moieties and the repulsion between membranes.

Recently, we have studied the lyotropic phase behavior of diene lipids,<sup>3,4,13</sup> which attract considerable interest because they can stabilize lipid structures by means of polymerization.<sup>14–17</sup> The polymerized lipids are cross-linked by covalent bonds which suppress individual and collective motions of the molecules.<sup>18</sup> In this study we will compare the hydration properties and the dimensions of bilayers of lipids with terminal diene groups possessing either phosphatidylcholine (PC) or phosphatidylethanolamine (PE) headgroups in the monomeric and in the

\* To whom correspondence should be addressed. E-mail: binder@rz.uni-leipzig.de. Fax: +49-341-9732479.

<sup>†</sup> Universität Leipzig.

<sup>‡</sup> Katholieke Universiteit Leuven.

(1) Cevc, G.; Marsh, D. *Phospholipid Bilayers: Physical Principles and Models*; John Wiley and Sons: New York, 1987.

(2) Parsegian, V. A.; Fuller, N.; Rand, R. P. *Proc. Natl. Acad. Sci. U.S.A.* **1979**, *76*, 2750.

(3) Binder, H.; Anikin, A.; Kohlstrunk, B.; Klose, G. *J. Phys. Chem. B* **1997**, *101*, 6618.

(4) Binder, H.; Anikin, A.; Lantsch, G.; Klose, G. *J. Phys. Chem. B* **1999**, *103*, 461.

(5) Gawrisch, K.; Parsegian, V. A.; Hajduk, D. A.; Tate, M. W.; Gruner, S. M.; Fuller, N. L.; Rand, R. P. *Biochemistry* **1992**, *31*, 2856.

(6) Hsieh, C.-H.; Sue, S.-C.; Lyu, P.-C.; Wu, W.-G. *Biophys. J.* **1997**, *73*, 870.

(7) Le Neveu, D. M.; Rand, R. P.; Parsegian, V. A. *Nature* **1976**, *259*, 601.

(8) Rand, P. *Annu. Rev. Biophys. Bioeng.* **1981**, *10*, 277.

(9) Rand, R. P.; Parsegian, V. A. *Biochim. Biophys. Acta* **1989**, *988*, 351.

(10) Israelachvili, J. N.; Wennerström, H. *Langmuir* **1990**, *6*, 873.

(11) Israelachvili, J. N.; Wennerström, H. *J. Phys. Chem.* **1992**, *96*, 520.

(12) Parsegian, V. A.; Rand, R. P. *Langmuir* **1991**, *7*, 1299.

(13) Binder, H.; Gutberlet, T.; Anikin, A.; Klose, G. *Biophys. J.* **1998**, *74*, 1908.

(14) Binder, H.; Anikin, A.; Kohlstrunk, B. *J. Phys. Chem. B* **1999**, *103*, 450.

(15) Srisiri, W.; Sisson, T. M.; O'Brien, D. F. O.; McGrath, K. M.; Han, Y.; Gruner, S. M. *J. Am. Chem. Soc.* **1997**, *119*, 4866.

(16) Lee, Y.-S.; Yang, J.-Z.; Sisson, T. M.; Frankel, D. A.; Gleeson, J. T.; Aksay, E.; Keller, S. L.; Gruner, S. M.; O'Brien, D. F. *J. Am. Chem. Soc.* **1995**, *117*, 5573.

(17) Chupin, V. V.; Anikin, A. V.; Serebrennikova, G. A. *Biol. Mem.* **1994**, *7*, 213.

(18) Anikin, A.; Chupin, V.; Anikin, M.; Serebrennikova, G.; Tarahovsky, J. *Makromol. Chem.* **1993**, *194*, 2663.

polymerized state. We expect to filter out the effects that exert molecular motions on the interbilayer repulsion. In a more general context, the present work is devoted to the characterization of the elastic properties of membrane stacks in terms of hydration force and lateral compressibility before and after polymerization using the osmotic stress technique.

A second aim of this work is motivated by our finding that terminal diene groups promote the formation of the inverse hexagonal,  $H_{II}$  phase.<sup>4</sup> This surprising property should be related to the increased curvature strain in membranes of diene lipids when compared with bilayers of lipids with saturated hydrocarbon chains. We will therefore pay attention to the dimensions of the  $H_{II}$  phase of monomeric bis(tetradecadienyl)phosphorylethanolamine to get insight into the specific influence of terminal diene groups on the properties of lipid aggregates.

The basic results were obtained by means of X-ray diffraction in combination with gravimetry to characterize the dimensions of the lipid aggregates at progressive dehydration. IR spectroscopy was used as an independent method to evaluate the degree of lateral compression of the hydrophobic core of the membranes. Details of the methods and some of the specific properties of the lipids bis(tetradecadienyl)phosphorylcholine (DTDPC) and -phosphorylethanolamine (DTDPE) have been described previously.<sup>4,13,14,18,19</sup>

## 2. Materials and Methods

**Materials.** 1,2-Bis(11,13-tetradecadienyl)-*sn*-glycero-3-phosphorylcholine (DTDPC) and 1,2-bis(11,13-tetradecadienyl)-*sn*-glycero-3-phosphorylethanolamine (DTDPE) were synthesized as described previously.<sup>4,18</sup> The purities of the lipids were confirmed by thin-layer chromatography. Stock solutions (chloroform/methanol: 3:1 v/v; 5 mg/mL) of the lipids were used for sample preparation. DLPE (dilauroyl-PE), DMPE (dimyristoyl-PE), and DPPE (dipalmitoyl-PE) were purchased from Sigma (Deisenhofen, Germany).

**Gravimetric Measurements.** The lipid in a stock solution (~0.5 mL) was spread on the surface of a circular quartz slide (diameter ~13 mm) and allowed to dry under a stream of nitrogen. The strip was placed into a twin microbalance system (Sartorius, Göttingen, Germany), which has been equipped with a moisture-regulating device (HumiVar, Leipzig, Germany; see also ref 3). The relative humidity, RH, was adjusted by flowing definitely moistened, high-purity  $N_2$  gas through the sample chamber. Before the experiments are started, the lipid has been dried for 12–24 h at RH = 0% until the mass of the sample attained some constant value (~0.5 mg). Adsorption isotherms were recorded in the continuous mode by scanning the RH continuously throughout the range RH = 5–98% with a rate of less than 10%/h. The samples were investigated by means of increasing (hydration scans) as well as decreasing (dehydration scans) RH at constant temperature,  $T$  ( $\pm 0.2$  K). The absence of hysteresis effects indicates that the samples were retained in thermodynamic equilibrium.

**X-ray Measurements.** For X-ray investigations a lipid film was spread on glass slides (20 × 25 mm) and dried. The slides were positioned into a sealed thermostated ( $\pm 0.5$  K) chamber mounted at a conventional Philips PW3020 powder diffractometer (Philips, Almelo, The Netherlands). X-ray powder diffractograms were obtained with Ni-filtered  $Cu K\alpha$  radiation (20 mA and 30 kV) by  $2\theta$  scans monitoring the range of reciprocal Bragg spacings  $s = (0.1 - 1.1) \text{ nm}^{-1}$  ( $s = 2 \sin \theta / \lambda$ ,  $\lambda = 0.15418 \text{ nm}$ ). The intensity was detected with a proportional detector system. Nitrogen of definite RH was continuously streamed through the sample chamber using a moisture-regulating unit (see above). The samples were investigated at discrete RH values and equilibrated for at least 4 h before measurements. Repeat distances are

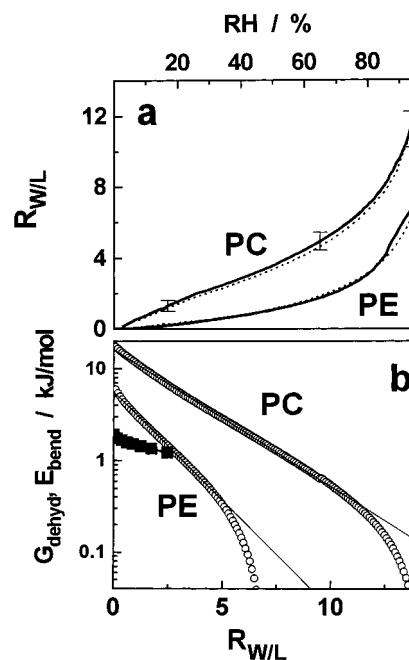


**Figure 1.** Adsorption isotherms of diene lipids before (solid lines) and after (dotted) polymerization (part a) and the free energy of dehydration,  $G_{\text{dehyd}}$ , of DTDPC and DTDPE as a function of the number of water molecules per lipid,  $R_{W/L}$ . The solid squares in part b show the bending energy,  $E_{\text{bend}}$ , of (hypothetical) monolayers of DTDPE at 45 °C (see below).

determined with an accuracy of  $\pm 0.1$  nm using the Bragg peaks of first order.

**Infrared Measurements.** Samples were prepared by spreading the lipid films on a ZnSe-attenuated total reflection (ATR) crystal (50 × 5 mm; face angle 45°). Polarized infrared spectra were recorded using a BioRad FTS-60a Fourier transform infrared spectrometer (Digilab, Cambridge, MA) and a horizontal Benchmark unit (Specac, Kent, U.K.) modified in order to realize a definite RH and temperature at the crystal surface coated with the lipid.<sup>3</sup> Band positions were calculated by means of the center of gravity.

IR reflection-absorption spectroscopy (IRRAS; see ref 20) was performed by placing a thermostated home-built Langmuir trough (220 × 26 mm) in the external beam using a reflection attachment of Specac (U.K.). The angle of incidence was 30°. After the lipid was spread from a chloroform solution, the area was reduced stepwisely with a compression velocity of 0.01  $\text{nm}^2 \cdot (\text{molecule} \cdot \text{min})^{-1}$ . Before an IRRAS spectrum (4096 scans, 2  $\text{cm}^{-1}$  resolution) was accumulated, the film was allowed to relax for 5 min.

**Polymerization.** Lipid films on a solid support (see above) were polymerized in a reaction chamber at a definite temperature and relative humidity. The films were illuminated through a quartz window using a UV lamp (4 W), which has been placed at a distance of ~3 cm from the lipid film. The irradiation time of 4 h was chosen to ensure complete transformation into the polymer in accordance with our previous studies on the kinetics of the polyreaction.<sup>14</sup>

## 3. Results and Discussion

**Water Adsorption Characteristics.** Figure 1 depicts the adsorption isotherms of DTDPC and DTDPE before and after UV polymerization. The shape of the isotherms of both lipids differs in a typical fashion that has been reported previously for lipids with PE and PC headgroups.<sup>21</sup> According to the classification scheme of multimolecular adsorption isotherms,<sup>22</sup> PC lipids exhibit a

(20) Dluhy, R. A. *J. Phys. Chem.* **1986**, *90*, 1373.

(21) Jendrasiak, G. L.; Hasty, J. H. *Biochim. Biophys. Acta* **1974**, *337*, 79.

(19) Binder, H.; Gutberlet, T.; Anikin, A. *J. Mol. Struct.* **1999**, in press.

**Table 1.** BET Parameters,  $R_{W/L}^1$  and  $RT \ln c$ , and Decay Characteristics of the Free Enthalpy of Dehydration,  $G_0$  and  $R_{W/L}^0$ , of the Water Adsorption Isotherms of DTDPE and DTDPC. The respective parameters of monomeric and polymerized lipids are equal within the error limits

	BET		$G_{\text{dehyd}}$	
	$R_{W/L}^1$	$RT \ln c / \text{kJ} \cdot \text{mol}^{-1}$	$G_0 / \text{kJ} \cdot \text{mol}^{-1}$	$R_{W/L}^0$
DTDPC	$2.2 \pm 0.2$	$5.2 \pm 0.3$	$16 \pm 2$	$2.9 \pm 0.3$
DTDPE	$1.3 \pm 0.2$	$1.3 \pm 0.3$	$5.6 \pm 0.8$	$1.8 \pm 0.3$

BET type IV (or II) characteristic and PE lipids a type V (or III) characteristic.<sup>21,23</sup> We used the BET equation in the linear form

$$\frac{a_W}{(1 - a_W)R_{W/L}} = \frac{1 + (c - 1)a_W}{R_{W/L}^1 c} \quad (1)$$

and plotted the left-hand side of eq 1 versus the water activity,  $a_W = \text{RH}/100$  (data not shown). Linear regression in the intermediate RH range,  $25\% < \text{RH} < 55\%$ , yields the molar ratio water/lipid at so-called monolayer coverage of the adsorbate,  $R_{W/L}^1$ , and the parameter  $c$  which is related exponentially to the enthalpy of adsorption in the first adsorbed layer.<sup>24</sup> The smaller BET parameters of DTDPE indicate the weaker water binding to the PE headgroups (cf. Table 1). No significant effect of polymerization on lipid hydration could be detected.

The free enthalpy of lipid dehydration can be evaluated in a model-independent way by means of<sup>25</sup>

$$G_{\text{dehyd}}(R_{W/L}) = \int_{a_W=1}^{a_W} \Delta\mu_W dR_{W/L}(a_W) \quad (2)$$

where  $\Delta\mu_W = \mu_W(a_W) - \mu_W(1)$  denotes the difference between the chemical potentials of water of activity  $a_W$  and 1 (saturated vapor and bulk water). The chemical potential difference of the water sorbed onto the lipid,  $\Delta\mu_W(R_{W/L})$ , is equal to that of the vapor,  $\ln a_W$ , because the water molecules can freely exchange between the lipid and the gas phases, i.e.

$$\Delta\mu_W = RT \ln a_W \quad (3)$$

$G_{\text{dehyd}}(R_{W/L})$  represents a measure of the work to dehydrate lipid partially. The free enthalpy of lipid dehydration can be fairly well approximated in a wide range of  $R_{W/L}$  by an exponential function,  $G_{\text{dehyd}}(R_{W/L}) \approx G_0 \exp(-R_{W/L}/R_{W/L}^0)$ . Linear regressions of  $\ln(G_{\text{dehyd}}(R_{W/L}))$  as a function of  $R_{W/L}$  yield the free enthalpy of complete dehydration,  $G_0$ , and a characteristic number of water molecules per lipid,  $R_{W/L}^0$  (cf. Figure 1, part b, and Table 1).

It is well-known that PC headgroups are highly hygroscopic whereas PE groups are more difficult to hydrate. At a low level of hydration direct H bonds between the phosphate and ammonium groups replace water-PE headgroup contacts and consequently lead to the stronger dehydration of the PE lipids when compared with phosphatidylcholines.<sup>4,26</sup> Hence, the terminal diene groups and the polymerization reaction obviously exert only a weak influence on the hydration characteristics of the lipids.

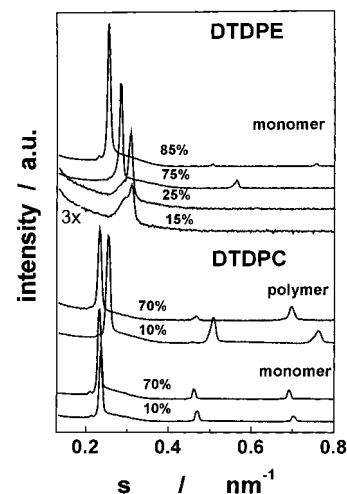


**Figure 2.** Representative X-ray diffraction patterns of DTDPE and DTDPC (monomeric and polymerized at  $T = 25^\circ\text{C}$  and  $\text{RH} = 50\%$ ) which were measured at different RHs (see figure) and temperatures (DTDPC,  $25^\circ\text{C}$ ; DTDPE,  $45^\circ\text{C}$ ). DTDPC exists exclusively in the  $L_\alpha$  phase at  $T = 25^\circ\text{C}$ .

As expected, their water adsorption potency is mainly determined by the polar moieties, i.e., the PE or PC headgroups.

**X-ray Diffraction Pattern of Lipid Films before and after Polymerization.** Figure 2 shows selected diffraction patterns of the diene lipids at selected RH and temperature values. The equally spaced Bragg reflections of DTDPC at all conditions studied and of DTDPE at  $\text{RH} = 85\%$  indicate the lamellar arrangement of the molecules. The  $\text{RH}-T$  phase diagram of DTDPE has been recently established using  $^{31}\text{P}$  NMR and IR linear dichroism measurements.<sup>4</sup> This lipid was found to exist in the  $H_{II}$  phase at  $T > 30-40^\circ\text{C}$  and  $\text{RH} < 80\%$ . The distinct shift of the Bragg reflections of DTDPE taking place between  $\text{RH} = 85\%$  and  $75\%$  ( $T = 45^\circ\text{C}$ ) indicates the  $L_\alpha/H_{II}$  phase transition in agreement with our previous findings.

A shoulder appears at the left-hand flank of the Bragg peak of first order of DTDPE at  $\text{RH} < 30\%$  which progressively protrudes upon further dehydration. This effect is possibly caused by the deformation of the circular cross section of the water cylinders at nearly dry conditions where direct interactions between the PE headgroups and sterical restrictions of headgroup packing come progressively into play. The hexagonal arrangement of the inverted cylinders seems to distort into ribbons in an oblique lattice.<sup>27,28</sup> Such, so-called ribbon phases have been reported to occur in almost dry DPPE, DPPC, and DOPE.<sup>25,29,30</sup> For the analysis in terms of geometric parameters, we will neglect this effect (see below).

Equally spaced Bragg reflections are also observed in films of DTDPC after UV irradiation. Hence, the polymerized lipid exists in a lamellar arrangement in agreement with previous results.<sup>14,18</sup> The same result was obtained when polymerizing DTDPE at conditions at which the monomeric lipid exists in the lamellar phase (not shown). The polymer shows no phase transformations.<sup>14</sup> Polymerization of DTDPE in the  $H_{II}$  phase yields no unequivocal results. The corresponding Bragg reflections typically represent doublets which can be interpreted as the

(22) Brunauer, S. *The Adsorption of Gases and Vapors*; Princeton University Press: Princeton, NJ, 1943; Vol. 1.

(23) Jendrasiak, G. L.; Smith, R. L.; Shaw, W. *Biochim. Biophys. Acta* **1996**, *1279*, 63.

(24) Sing, K. S. W.; Everett, D. H.; Haul, R. A. W.; Moscou, L.; Pierotti, R. A.; Rouquerol, J.; Siemieniowska. *Pure Appl. Chem.* **1985**, *57*, 603.

(25) Cevc, G. Lipid hydration. In *Water and Biological Macromolecules*; Westhof, E., Ed.; CRC Press: Boca Raton, FL, 1993; p 368.

(26) Hitchcock, P. B.; Mason, R.; Thomas, K. M.; Shipley, G. G. *Proc. Natl. Acad. Sci. U.S.A.* **1974**, *71*, 3036.

(27) Seddon, J. M. *Biochim. Biophys. Acta* **1990**, *1031*, 1.

(28) Tardieu, A.; Luzzati, V.; Reman, F. C. *J. Mol. Biol.* **1973**, *75*, 711.

(29) Jürgens, E.; Höhne, G.; Sackmann, E. *Ber. Bunsen-Ges. Phys. Chem.* **1983**, *87*, 95.

(30) Pohle, W.; Selle, C. *Chem. Phys. Lipids* **1996**, *82*, 191.

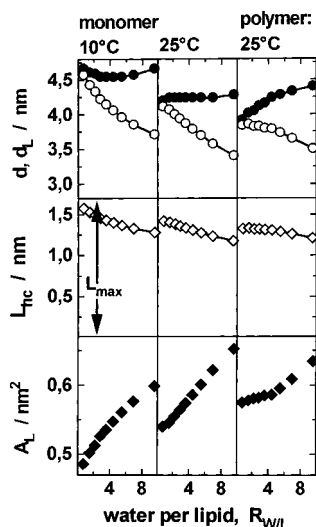


**Figure 3.** Dimensions of monomeric and polymeric DTDPC bilayers as a function of hydration at different temperatures. The polymerization has been realized in the  $L_{\alpha}$  phase of the monomeric lipids ( $T = 25^{\circ}\text{C}$ ,  $\text{RH} = 50\%$ ). The geometric parameters of the multilamellar stacks are defined as follows (see also Figure 9, part A, for illustration): repeat distance  $d$  (●); thickness of the bilayer  $d_L = d - d_W$  (○); area per lipid  $A_L = 2(v_L + R_{W/L}v_W)/d$  (◆); thickness of the water layer  $d_W = 2R_{W/L}v_W/A_L$ ; thickness of the polar part of the bilayer  $d_{\text{pol}} = 2v_{\text{pol}}/A_L$ ; thickness of the hydrophobic core  $d_{\text{hc}} = d_L - d_{\text{pol}}$  (see, e.g., ref 31).  $v_{\text{pol}}$  denotes the volume of the nonhydrated polar part of the lipids which includes the glycerol and carbonyl moieties. For the PC and PE lipids we used the values proposed by Scherer,<sup>34,52</sup>  $v_{\text{pol}} = 0.344 \text{ nm}^3$  and  $0.246 \text{ nm}^3$ , respectively.  $L_{\text{hc}} = 0.5d_{\text{hc}}$  is the thickness of the hydrophobic core of half of the bilayer (◇). The double arrow illustrates the length of an extended tetradecadienyl chain in the all-trans conformation,  $L_{\text{max}} = 1.65 \text{ nm}$ .

superposition of two lamellar structure or, alternatively, of a lamellar and a hexagonal structure. Stable polymerized  $H_{\text{II}}$  hexagons were obtained recently by redox-initiated radical polymerization of lipids with diene groups in a position adjacent to the carbonyl moieties.<sup>15</sup> The influence of factors such as the position of the diene groups and/or the type of initiation of the polymerization reaction will be studied separately. Here, we deal with monomeric and polymerized lamellae of both lipids and with the  $H_{\text{II}}$  phase of the DTDPE monomers.

**Dimensions of the Lipid Aggregates.** The geometric parameters of the lamellar and hexagonal phases of the diene lipids were estimated within the framework of the approach of nonpenetrating lipid/water volumes proposed by Luzzati<sup>31</sup> using the amount of water which is sorbed to the samples at different RH (see Figures 3 and 4; the geometric parameters are assigned in the legends).

In the  $L_{\alpha}$  phase ( $T = 25^{\circ}\text{C}$ ) the DTDPC molecules occupy an area of  $A_L \approx 0.55\text{--}0.65 \text{ nm}^2$  within the membrane plane. At  $10^{\circ}\text{C}$  and  $R_{W/L} < 4$ , the lipid undergoes the phase transition into the gel upon dehydration.<sup>19</sup> The smaller cross-sectional area of the all-trans polymethylene segments gives rise to the reduction of  $A_L$  to  $\sim 0.49\text{--}0.55 \text{ nm}^2$ . The length of the  $\text{CH}_2=\text{CH}-\text{CH}=\text{CH}-(\text{CH}_2)_9$ -fragment of the tetradecadienyl chain in the all-trans conformation,  $L_{\text{max}} \approx 1.65 \text{ nm}$ , was estimated using standard bond lengths and angles.<sup>32,33</sup> The thickness of

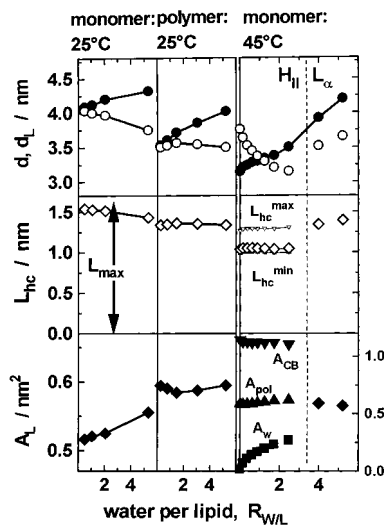


**Figure 4.** Dimensions of the lamellar and inverse hexagonal phase of DTDPE as a function of hydration at different temperatures. Polymerized bilayers were obtained by UV irradiation of monomeric bilayers ( $T = 25^{\circ}\text{C}$  and  $\text{RH} = 50\%$ ). The vertical dashed line in the right part indicates the  $H_{\text{II}}/L_{\alpha}$  phase transition. The dimensions of the bilayers are assigned in the caption of Figure 3. The dimensions of the  $H_{\text{II}}$  phase are defined as follows (see also Figure 9, parts A and C): repeat distance  $d$  (●); mean thickness of the hydrophobic part perpendicular to the cylinder axes  $d_L = 2((2\pi\sqrt{3})^{0.5}d - r_W)$  (○); area per lipid at the cell boundary  $A_{\text{CB}} = 2\sqrt{3}(v_L + R_{W/L}v_W)/d$  (▼); area per lipid at the water/lipid boundary  $A_W = (v_W/d) - (2\sqrt{3}/\phi_W)^{0.5}$  (▲); area per lipid at the polar/apolar boundary  $A_{\text{pol}} = (v_{\text{pol}}/d)(2\sqrt{3}/\phi_{\text{pol}})^{0.5}$  (■); radius of the water (or the polar) cylinders  $r_{W,\text{pol}} = d(2\phi_{W,\text{pol}}/\pi\sqrt{3})^{0.5}$ ; minimum, maximum, and mean thicknesses of the hydrophobic region of the curved monolayer  $L_{\text{hc}}^{\text{min}} = (d\sqrt{3} - r_{\text{pol}})$  (–);  $L_{\text{hc}}^{\text{max}} = (2d/3 - r_{\text{pol}})$  (▽) and  $L_{\text{hc}} = L_{\text{hc}}^{\text{min}}(2\sqrt{3}/\pi)^{0.5}$  (◇), respectively.  $\phi_W$  and  $\phi_{\text{pol}}$  are the volume fractions of the water and of the water plus the polar part of the lipids, respectively (see, e.g., refs 27 and 44).

the hydrophobic core of half of the bilayer in the gel state of DTDPC,  $L_{\text{hc}} \approx 1.5\text{--}1.6 \text{ nm}$ , is slightly smaller than  $L_{\text{max}}$  (Figure 3, middle). DTDPE exists predominantly in the gel phase at  $25^{\circ}\text{C}$ .<sup>4</sup> The corresponding  $A_L$  and  $L_{\text{hc}}$  values agree with those of DTDPC (compare Figures 3 and 4). The smaller volume of the PE headgroup gives, however, rise to a decreased repeat distance,  $d$ , of DTDPE.

The Bragg reflections of polymerized DTDPC shift considerably at progressive hydration, whereas the positions of the diffraction peaks of monomeric DTDPC virtually remain unchanged (Figure 2). A similar tendency has been found to occur for the diffraction pattern of the lamellar phase of DTDPE before and after polymerization (not shown). The analysis within the framework of the Luzzati model reveals that the area of the polymerized lamellae is essentially constant upon increasing hydration, whereas  $d$  increases considerably. Hence, the accumulation of water between the lipid layers causes mainly the swelling of the interbilayer gap. On the other hand, the water volume between the bilayers of monomeric lipid expands predominantly parallel to the surface by means of a lateral expansion of the lamellae, and thus  $d$  changes only little throughout the RH range studied.

In the  $H_{\text{II}}$  phase of DTDPE the repeat distance,  $d$ , and the mean thickness of the hydrophobic region of the curved monolayers,  $L_{\text{hc}}$ , are distinctly reduced in comparison with the respective parameters of the lamellar phase (cf. the right part of Figure 3 and Figure 9, part B, for illustration). Only the maximum length,  $L_{\text{hc}}^{\text{max}} \approx 1.3 \text{ nm}$ , in which the acyl chains must stretch to fill the interstitial spaces agrees

(31) Luzzati, V. *X-ray diffraction studies of lipid-water systems*; Academic Press: London, 1968; Vol. 1.

(32) Orchard, B. J.; Tripathy, S. K.; Hopfinger, A. J.; Taylor, P. L. *J. Appl. Phys.* **1981**, *52*, 5949.

(33) Tanford, C. *The hydrophobic effect*; Wiley and Sons: New York, 1973.

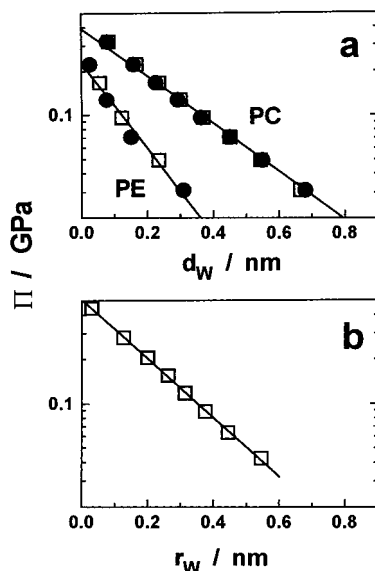


**Figure 5.** Hydration pressure,  $\Pi$ , as a function of the distance between opposite bilayers,  $d_W$  (a), and of  $r_W$ , the radius of the water cylinders in the  $H_{II}$  phase (b). Monomeric ( $\square$ ) and polymerized ( $\bullet$ ) DTDPC and DTDPE at 25 °C (a) and monomeric DTDPE at 45 °C (b). The slopes and intercepts,  $\lambda^{-1}$  and  $\Pi_0$ , respectively, of the linear regressions (lines) are listed in Table 2.

with the thickness of the hydrophobic core of the lamellar monolayers in the  $L_\alpha$  phase. The smaller dimensions of the hydrophobic core in the  $H_{II}$  phase can be partially explained by the increased conformational disorder of the acyl chains which becomes evident, e.g., from the slight increase of the position of the  $CH_2$  stretching bands in the IR spectrum at the  $L_\alpha/H_{II}$  phase transition.<sup>4</sup> On the other hand, the small values of  $L_{hc}$ , and especially of  $L_{hc}^{min}$ , suggest the partial interdigitation of the hydrocarbon chains in the region of the terminal diene groups (see below and Figure 9 for illustration). This hypothesis is confirmed by the mean area per molecule on the Wigner–Seitz cell boundary,  $A_{CB} \approx 1.11 \text{ nm}^2$ , which amounts to nearly twice the area at the position of the polar/apolar interface,  $A_{pol} \approx 0.60 \text{ nm}^2$  (Figure 4). The same conclusion was drawn by Scherer on the basis of geometrical data of  $H_{II}$  aggregates of disaturated PEs.<sup>34</sup>

The lipid monolayers which surround the water cylinders “unbend” at the  $H_{II}/L_\alpha$  phase transition. That means the polar part of the lipid expands whereas the hydrocarbon terminus is compressed in the direction perpendicular to the molecular long axes.  $A_{pol}$  remains essentially constant, and consequently this position along the DTDPE molecules can be interpreted as their pivotal position.<sup>35</sup> Interestingly, the variation of the amount of sorbed water has only a small effect on the dimensions of the hydrophobic region of the  $H_{II}$  aggregates.

**Repulsive Forces between Hydrophilic Interfaces.** Semilogarithmic plots of the hydration pressure<sup>9</sup>

$$\Pi = -\Delta\mu_W/v_W \quad (4)$$

as a function of  $d_W$ , the thickness of the water gap between the surfaces of opposite lipid layers, yield the decay length,  $\lambda$ , of the repulsive forces between the membranes (see Figure 5 and Table 2). The substitution of the ammonium group in the polar heads of DTDPE for the trimethylam-

**Table 2.** Decay Length,  $\lambda$ , Hydration Pressure,  $\Pi_0$ , Work of Complete Dehydration,  $G_0$ , and the Area per Lipid,  $A_{min}$ , at the Polar/Apolar Interface of the Dehydrated Lipid Aggregates

lipid	$\Pi$ °C	$\lambda$ / nm <sup>a</sup>	$\Pi_0$ / GPa <sup>a</sup>	$A_{min}$ / nm <sup>2</sup>	$G_0$ / kJ·mol <sup>-1</sup> <sup>b</sup>
DTDPC	monomer (gel)	10	0.28	0.40	17
	monomer ( $L_\alpha$ )	25	0.26	0.42	18
	polymer	25	0.27	0.39	18
DTDPE	monomer (gel)	25	0.15	0.23	5
	polymer	25	0.15	0.23	6
	monomer ( $H_{II}$ )	45	0.22	0.51	5

<sup>a</sup> According to  $\Pi = \Pi_0 \exp(-d_W/\lambda)$  or  $\Pi = \Pi_0 \exp(-r_W/\lambda)$ , see Figure 5. <sup>b</sup> According to eq 5 and  $G_0^{lam}$  and  $G_0^{hex}$  (see text). <sup>c</sup> SE:  $\pm 0.03$  ( $\lambda$ ),  $\pm 0.1$  ( $\Pi_0$ ),  $\pm 0.02$  ( $A_{min}$ ),  $\pm 1$  ( $G_0$ ) in units given in the table.

monium group in DTDPC results in a significant increase of the decay length in accordance with previous findings.<sup>9</sup> This tendency and the increased pressure,  $\Pi_0$ , which is necessary to bring opposite PC layers into close contact reflect the bigger hydration potency of the PC moieties (vide supra).

Individual and collective motions of the lipid molecules potentially cause undulation, protrusion, and peristaltic forces in the liquid-crystalline membranes of monomeric lipids.<sup>11,36</sup> At least the mobility of individual molecules will be strongly suppressed in the polymerized membranes owing to the existence of intermolecular covalent bonds. Note that the lateral compressibility within the polymerized lamellae is drastically reduced in comparison with the monomeric membranes (see below). The repulsive forces between the DTDPE and DTDPC bilayers remain, however, unaffected by the polymerization reaction (see Figure 5, part a). We conclude that the hydration force is mainly caused by the solvation properties of the polar moieties of the lipids in the RH range investigated.

This finding is in contradiction to that of Gordelij et al.,<sup>37</sup> who compared X-ray data of DTDPC and DMPC (dimyristoyl-PC) membranes. The authors stated to polymerize their membranes under X-ray. We found no degradation of the diene groups after our X-ray experiments, as has been proved by IR spectroscopy (see ref 14 for details). Furthermore, Gordelij et al. interpreted the small changes of the repeat distance,  $d$ , in their DTDPC samples in terms of a short decay length of the hydration force (0.07 nm). This analysis disregards the considerable lateral deformation of the multilamellar samples of the diene lipids, which we proved independently by IR spectroscopy (see below).

**Free Enthalpy of Dehydration.** Combination of eqs 2–4 yields the free energy of complete dehydration as a function of the dimensions of the lipid aggregates by integrating the hydration pressure over the change of the water volume:<sup>2</sup>

$$G_0 = -\frac{1}{2}N_A \int_{\infty}^0 \Pi dV_W \quad (5)$$

Making use of  $dV_W \approx A_{min} d(d_W)$  and expressing  $\Pi$  in terms of the exponential decay law established empirically for the dehydration of the lipid lamellae, one obtains after integration  $G_0^{lam} \approx 0.5N_A P_0 \lambda A_{min}$  where  $A_{min}$  denotes the area per lipid in the almost dehydrated lamellae.<sup>9</sup>

Interestingly, also a semilogarithmic plot of the hydration pressure as a function of the radius of the water

(34) Scherer, J. R. *Biophys. J.* **1989**, *55*, 957.

(35) Rand, R. P.; Fuller, N. L.; Gruner, S. M.; Parsegian, V. A. *Biochemistry* **1990**, *29*, 76.

(36) Helfrich, W. Z. *Naturforsch.* **1978**, *33a*, 305.

(37) Gordelij, V. I.; Cherezow, V. G.; Anikin, A. V.; Anikin, M. V.; Chupin, V. V.; Teixeira, J. *Prog. Colloid Polym. Sci.* **1996**, *100*, 338.

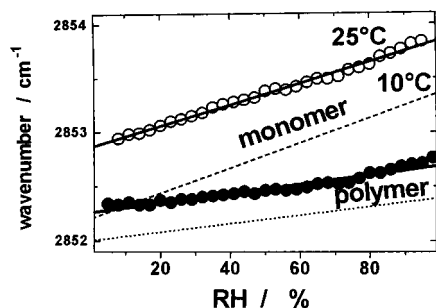


**Figure 6.** Center of gravity of the infrared adsorption band of the symmetric stretching vibration of the methylene groups of monomeric and polymerized DTDPc as a function of the relative humidity, RH, at 25 and 10 °C. The polymerization has been realized in the  $L_\alpha$  phase ( $T = 25$  °C and  $RH = 50\%$ ) of the monomer. The slope of the regression lines is  $\sim 1 \times 10^{-3} \text{ cm}^{-1}/\%$  (monomer) and  $\sim 0.4 \times 10^{-3} \text{ cm}^{-1}/\%$  (polymer). Experimental points are omitted for the data which have been measured at 10 °C. Only data which correspond to the  $L_\alpha$  phase of DTDPc were considered.

cylinders in the  $H_{II}$  phase,  $r_W$ , reveals a linear relation (Figure 5, part b, and Table 3). Consequently, one can calculate the free enthalpy of dehydration from the dimensions of the  $H_{II}$  phase using eq 5 and  $\Pi = \Pi_0 \exp(-r_W/\lambda)$ . The volume change of water cylinders per lipid molecule is given by  $dV_W = 2\pi b r_W dr_W + \pi r_W^2 db$ .  $b$  denotes the length of the water cylinders per lipid molecule. With  $db \ll dr_W$ , one obtains  $dV_W \approx 2\pi b r_W dr_W$ . Let us assume that the pivotal position of the molecules is located at the radius,  $r_{pol}$ , of a cylinder which makes the polar/apolar interface, i.e.,  $A_{pol} = \text{constant}$ . Let us further use the condition of incompressibility of the polar part of the lipids, i.e.,  $v_{pol} = \text{constant}$ . Then the combination of  $A_{pol} = 2\pi r_{pol} b = \text{constant}$  with  $v_{pol} = \pi(r_{pol}^2 - r_W^2)b = \text{constant}$  yields  $r_{pol} = (v_{pol}/A_{pol}) + \{(v_{pol}/A_{pol})^2 + r_W^2\}^{0.5}$ . Insertion into eq 5 gives the result

$$G_o^{\text{hex}} = \frac{1}{2} N_A \Pi_0 A_{pol} \int_{\infty}^0 \exp\left(-\frac{r_W}{r_{pol}}\right) dr_W \approx \frac{1}{4} N_A \Pi_0 \frac{(A_{pol} \lambda)^2}{v_{pol}} \quad (6)$$

The free energies of dehydration which were calculated from the dimensions of the lamellar and inverse hexagonal phases are listed in Table 2. They agree fairly well with the corresponding results of direct integration of the adsorption isotherms using eq 2 (cf. Table 1). The exponential decay laws of  $G_{\text{dehyd}}$  and of  $\Pi$  seem to reflect the solvation properties of the headgroups which obviously dominate the hydration behavior of the lipids in the RH range studied. Other factors, such as monolayer bending, require little osmotic work, and thus they seem to affect the free energy of complete dehydration only to a negligible extent (see below and ref 5). Note, for example, that the transition enthalpy of the  $H_{II}/L_\alpha$  phase transition of DTDPE ( $< 1 \text{ kJ/mol}^4$ ) is distinctly smaller than the  $G_o$  values.

**Methylene Stretching Frequencies and the Lateral Area.** The degree of molecular order within the hydrophobic core of lipid membranes can be well characterized using infrared spectroscopy. Figure 6 depicts the position of the symmetric methylene stretching band,  $\nu_s(\text{CH}_2)$ , of DTDPc before and after polymerization as a function of RH.  $\nu_s(\text{CH}_2)$  increases nearly linearly with RH. The slope of the polymer data is reduced by a factor of 2 in comparison with the slope of the corresponding monomer data (see the caption of Figure 6).

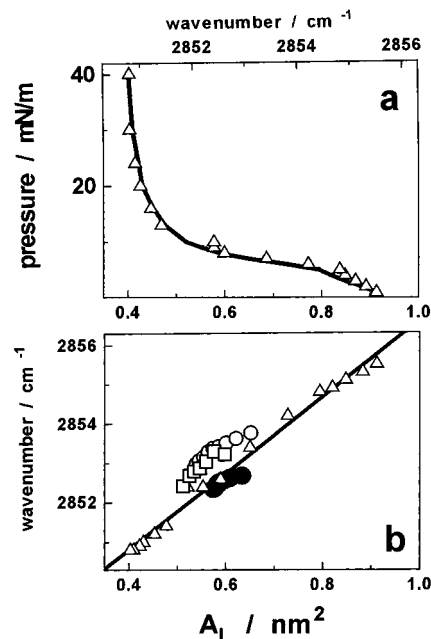


**Figure 7.** Surface pressure–molecular area ( $A_L$ ) isotherm for a DMPE monolayer at the water–air interface (part a, line,  $T = 25$  °C) and the corresponding wavenumbers of the  $\text{CH}_2$  symmetric stretching vibrations,  $\nu_s(\text{CH}_2)$ , as a function of the surface pressure ( $\Delta$ ). Part b depicts a correlation plot between these  $\nu_s(\text{CH}_2)$  data and  $A_L$ . Linear regression (line) yields a slope of  $\sim 9.7 \text{ cm}^{-1}/\text{nm}^2$ . The  $\nu_s(\text{CH}_2)$  values of bilayers of monomeric (10 °C,  $\square$ ; 25 °C,  $\circ$ ) and polymerized (25 °C) DTDPc are shown in part b as a function of  $A_L$ .

On the one hand, the frequency of the methylene stretching band,  $\nu_s(\text{CH}_2)$ , depends on the degree of conformational order of the acyl chains.<sup>4,38</sup> IR investigations of lipids at variable hydrostatic pressure show that, on the other hand, the frequency shift of  $\nu_s(\text{CH}_2)$  can be understood as an indication of the balance between repulsive and attractive contributions to the intermolecular potential of the methylene groups.<sup>39</sup> Consequently, the decrease of  $\nu_s(\text{CH}_2)$  with dehydration reflects at least two effects which are correlated to each other: (i) the increase of the conformational order of the polymethylene fragments of the tetradecadienoyl chains and (ii) the strengthening of attractive interactions between neighboring acyl chains. Both tendencies are caused by the lateral compression of the lipid aggregates upon increasing hydration pressure.

The spectral parameter,  $\nu_s(\text{CH}_2)$ , obviously correlates with the cross section of the lipid molecules within the membrane plane. We checked this hypothesis in a reference IRRAS experiment by means of gradual compression of lipid monolayers at the water–air interface. Part a of Figure 7 shows the surface pressure–area isotherm of DMPE at 20 °C and the corresponding positions of the  $\nu_s(\text{CH}_2)$  band. The wavenumbers run virtually parallel to the surface area per molecule,  $A_L$ . Similar results were obtained with DLPE and DPPE (not shown). Hence,  $\nu_s(\text{CH}_2)$  changes obviously proportional to  $A_L$  as confirmed by a regression coefficient of  $> 0.995$  (see Figure 7, part b). In Figure 7, part b, we also correlate the  $\nu_s(\text{CH}_2)$  frequencies of monomeric and polymerized DTDPc bilayers (cf. Figure 6) with the corresponding  $A_L$  values which were calculated from the X-ray data (Figure 3). The experimental points confirm the linear relation

(38) Kodati, V. R.; Lafleur, M. *Biophys. J.* **1993**, *64*, 163.

(39) Guo, J. D.; Zerda, T. W. *J. Phys. Chem. B* **1997**, *101*, 5490.

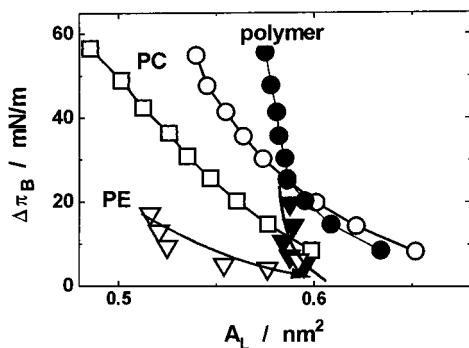


**Figure 8.** Lateral tension of lipid bilayers,  $\Delta\pi_B$ , in membranes of monomeric (open symbols) and polymeric (solid symbols) DTDPC (squares,  $T = 10^\circ\text{C}$ ; circles,  $T = 25^\circ\text{C}$ ) and DTDPE (down triangles,  $T = 25^\circ\text{C}$ ) as a function of the area per lipid,  $A_L$ . The experimental data were calculated by means of eq A5.

between  $\nu_s(\text{CH}_2)$  and  $A_L$ , which has been established on the basis of the monolayer experiment.

These results show that the wavenumber of the  $\text{CH}_2$  stretching vibration represents a measure of the area which the lipid molecules occupy within the membrane plane. Consequently, the different slopes of the  $\nu_s(\text{CH}_2)$  versus RH dependences of monomeric and polymerized membranes represent an independent indication of the different area change of both systems at lateral compression. Obviously, the intermolecular covalent bonds of the polymeric network in the membrane center fix adjacent molecules at a certain distance and thus impede or even prevent their closer approach upon dehydration. Note that temperature variation only weakly affects the RH increment of  $\nu_s(\text{CH}_2)$  (Figure 6).

The degree of molecular order within the polymerized membranes can be modulated by the phase state of the monomeric lipid at the beginning of the polyreaction.<sup>14</sup> In particular, we found that the  $\nu_s(\text{CH}_2)$  values of lipid films which were polymerized in the gel state are systematically smaller than that of films which were obtained by polymerization in the  $L_\alpha$  phase. We attributed this difference to a higher degree of acyl chain ordering in the former samples. The conditions of the polymerization reaction have, however, no measurable effect on the RH increment of  $\nu_s(\text{CH}_2)$  (not shown). We conclude that the compressibility of the polymerized membranes is mainly determined by the intermolecular covalent bonds and only to a negligible extent by the segmental order of the polymethylene chains.

**Lateral Compressibility of Monomeric and Polymerized Membranes.** Lipid bilayers are stabilized by the equilibrium between the repulsive lateral pressure within each of the monolayers,  $\pi$ , and the cohesive hydrophobic tension at the polar/apolar interface,  $\gamma$ , according to the principle of opposing forces.<sup>33</sup> The difference,  $\Delta\pi_B$ , of the lateral pressure between the fully hydrated, "relaxed" bilayer and the partially dehydrated bilayer under osmotic stress can be estimated using the thickness of the water layer, the decay length, and the hydration pressure (see Appendix A, eq A5). Figure 8 shows that the lateral pressure within the membranes of monomeric lipids decreases in the order DTDPC( $25^\circ\text{C}$ ) > DTDPC( $10^\circ\text{C}$ ) > DTDPE( $25^\circ\text{C}$ ) at  $A_L = \text{constant}$ . The difference of  $\Delta\pi_B$  between DTDPC at  $25^\circ\text{C}$  and that at  $10^\circ\text{C}$  can be explained by the reduced flexibility of the tetradecadienoyl chains in the gel state. The conformational freedom of the lipid hydrocarbon chains depends on the area per molecule, and therefore the associated free energy gives a repulsive contribution to the lateral

pressure which decreases in a more ordered membrane.<sup>40,41</sup> The difference of  $\Delta\pi_B$  between DTDPC and DTDPE can be attributed to the smaller volume of the PE headgroups which gives rise to a weaker repulsion between neighboring molecules.

In each system  $\Delta\pi_B$  increases continuously with decreasing area of the membrane (Figure 8). The slope of the curves yields the lateral compressibility modulus which is defined as

$$K_A = -A_L \left( \frac{\partial \Delta\pi_B}{\partial A_L} \right)_{T=\text{constant}} \quad (7)$$

In the monomeric bilayers  $K_A$  adopts values of 150–300 mN/m, which are typically measured in lipid bilayers using the osmotic stress technique<sup>13,42</sup> or micromechanical manipulation.<sup>43</sup> Hence, the terminal diene groups have no significant effect on the compressibility of the bilayers. The polymerized bilayers, however, become virtually incompressible at  $A_L < 0.58 \text{ nm}^2$  ( $K_A > 1500 \text{ mN/m}$ ) where repulsive forces between the lipid molecules increase drastically because of the polymeric network.

**Monolayer Bending Deduced from  $H_{II}$  Phase Dimensions.** Let us consider the lateral pressure,  $\pi$ , within a monolayer. It is convenient to consider the lateral pressure profile,  $p(z)$ , in the direction along the monolayer normal because  $\pi$  acts across the whole thickness of the lipid layer. The  $p(z)$  profile defines the components of the lateral pressure which are caused by the polar part and by the hydrocarbon chains of the lipids

$$\pi_{\text{pol}} = \int_0^{L_{\text{pol}}} p(z) dz \quad \text{and} \quad \pi_{\text{hc}} = \int_0^{L_{\text{hc}}} p(z) dz \quad (8)$$

respectively.  $L_{\text{pol}}$  and  $L_{\text{hc}}$  are the thicknesses of the polar and apolar parts of the monolayer, respectively. The moments of the pressure components  $\pi_{\text{pol}}$  and  $\pi_{\text{hc}}$  balance about its center of gravity at  $z = D$  according to

$$\int_0^{L_{\text{pol}}} (p(z)(z+D)) dz = \int_0^{L_{\text{hc}}} (p(z)(z-D)) dz \quad (9)$$

The lateral pressure of the monolayer,  $\pi = \pi_{\text{pol}} + \pi_{\text{hc}}$ , is compensated by the cohesive hydrophobic tension at the polar/apolar interface, i.e.,  $\pi = \gamma$ .<sup>1,33</sup> Hence,  $\gamma$  acts at  $z = 0$  and the balanced forces,  $\gamma$  and  $\pi$ , in the resultant couple are separated by  $D$  (see Figure 9, part B). Consequently,  $\pi$  and  $\gamma$  create the bending moment

$$M = -\pi D \quad (10)$$

$M$  induces a torque tension that tends to bend the monolayer into a structure with a spontaneous radius of curvature  $R_0 < 0$  ( $M > 0$ , inverse structures, "water inside") or  $R_0 > 0$  ( $M < 0$ , "water outside").

Usually,  $M$  increases upon dehydrating the lipids owing to the increase of the fraction of the lateral pressure of the hydrocarbon chains,  $f_{\text{hc}}$  (see eq B1, Appendix B). The monolayers are assembled in symmetrical bilayers, the net torque of which will be zero because the bending moments of the two monolayers will cancel. If the tendency to bend the monolayers is relatively strong, then the bilayer under intrinsic tension may no longer be the most stable state for the lipid assembly. At any critical value of the bending moment, the bilayers will transform into

(40) Marsh, D. *Biochim. Biophys. Acta* **1996**, *1286*, 183.

(41) De Young, L. R.; Dill, K. A. *Biochemistry* **1988**, *27*, 5281.

(42) Koenig, B. W.; Strey, H. H.; Gawrisch, K. *Biophys. J.* **1997**, *73*, 1954.

(43) Evans, E.; Needham, D. *J. Phys. Chem.* **1987**, *91*, 4219.

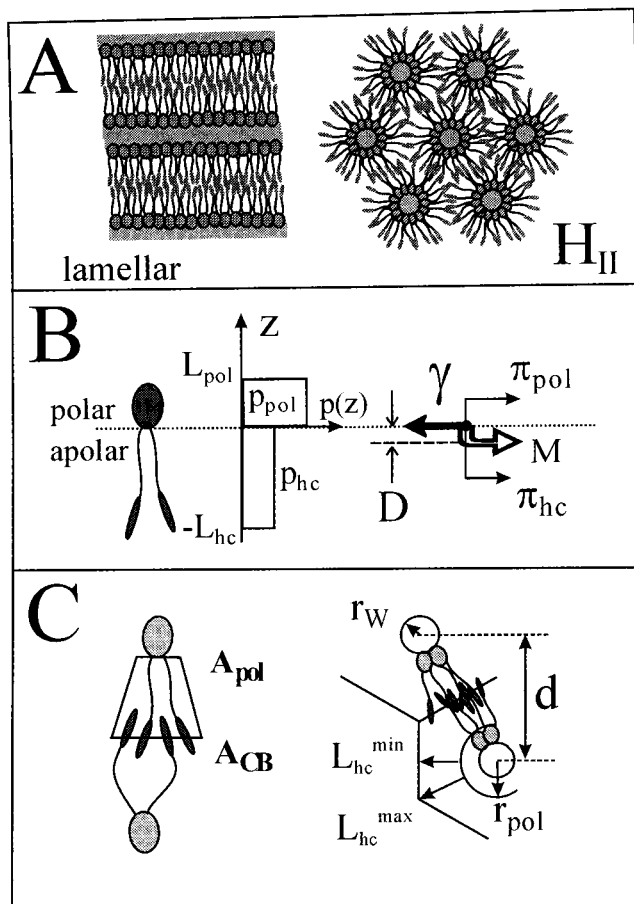


**Figure 9.** Schematic illustration of the structure of lipid aggregates (part A), of the components of the lateral pressure in membranes (part B), and of the geometry of the inverse hexagonal phase (part C). See the text for an explanation.

curved, monolayer-related structures such as the inverted hexagonal phase. This phase transition was really observed upon dehydrating DTDPE at 45 °C (see above and ref 4).

The curvature of the monolayers within the  $H_{II}$  hexagons expresses the frustrated spontaneous curvature of corresponding (hypothetical) DTDPE monolayers in the lamellar phase.<sup>44</sup> The center of gravity of the pressure components,  $D$ , the fraction of  $\pi_{hc}$ ,  $f_{hc}$ , the apparent bending modulus of the lipid monolayers,  $k_c$ , and the bending energy,  $E_b$ , can be estimated from the dimensions of the lipid cylinders in the  $H_{II}$  phase (cf. Appendix B). Figure 10 shows that the increasing fraction of the lateral pressure within the hydrophobic region is paralleled by the shift of the offset position of the lateral pressure,  $D$ , away from the pivotal position at the polar/apolar interface. The area requirement per molecule within the pivotal surface is nearly a constant,  $A_{pol} \approx 0.60 \text{ nm}^2$ , and equals, approximately, the area per lipid in the relaxed bilayer (cf the right part of Figure 4). The surface tension,  $\gamma$ , which balances the lateral pressure depends on the area of the hydrophobic/hydrophilic interface. It appears reasonable to assume that  $\gamma \approx 35 \text{ mN/m} = \text{constant}^1$  because of  $A_{pol} \approx \text{constant}$ . Consequently, the increase of  $D$  gives rise to an increasing bending moment of the monolayer,  $M$  (cf eq 10).

The apparent bending modulus,  $k_c$ , decreases with increasing  $r_{pol}$  from  $\sim 4.5 \text{ kJ/mol}$  at  $r_{pol} < 0.8$  to  $\sim 4.1 \text{ kJ/mol}$  at  $r_{pol} > 0.9 \text{ nm}$  (eq B3). These values agree with the

(44) Marsh, D. *Biochim. Biophys. Acta* **1996**, *1279*, 119.

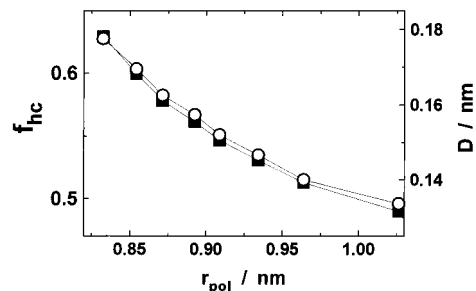


**Figure 10.** Fraction of the pressure of the hydrocarbon chains,  $f_{hc}$  (○), and offset distance of the lateral pressure,  $D$  (■), in membranes as deduced from the  $H_{II}$  phase dimensions of DTDPE at 45 °C as a function of the radius of the polar cylinders,  $r_{pol}$ .

bending moduli which are typically found for lipid monolayers.<sup>27</sup> Part b of Figure 1 depicts the corresponding bending energy,  $E_{bend}$  (cf. eq B5), together with the free energy of dehydration,  $G_{dehyd}$ . Both energies are equal ( $\sim 1.2 \text{ kJ/mol}$ ) at  $R_{W/L} \approx 2.5$ . At a higher degree of hydration,  $E_{bend}$  is expected to exceed  $G_{dehyd}$ ; i.e., the energetics of the lipid aggregates are increasingly determined by their elastic properties. This result is not surprising because it is known that the bending energy gives the leading contribution to the energetics of the inverse hexagonal phase at an intermediate and high level of hydration.<sup>3,35,45</sup>

**Why Do the Terminal Diene Groups Promote  $H_{II}$  Phase Formation?** The mean molecular shape of the hydrophobic part of the lipid molecules must possess a certain asymmetry to assemble into inverse hexagons. It can be imagined as a truncated cone with the face areas  $A_{pol}$  and  $A_{CB}$  (cf. Figure 9, part C). The relatively large volume in the center of the hydrophobic region can be filled if, e.g., the hydrocarbon chains possess a high degree of disorder. Therefore, factors that increase the conformational disorder of the hydrocarbon chains such as cis unsaturation and/or heating promote the formation of the  $H_{II}$  phase.<sup>35,46</sup> The  $L_{\alpha}/H_{II}$  phase transition temperature increases nearly linearly with decreasing effective chain length,  $n_{eff}$  (the number of carbon atoms in the chain), and exceeds 100 °C for fully hydrated disaturated PEs with  $n_{eff} < 14$  (alkyl chains) or with  $n_{eff} < 20$  (acyl chains).<sup>47,48</sup> This tendency illustrates the correlation between conformational disorder and  $H_{II}$ -phase formation because the degree of disorder within the hydrophobic core should increase with decreasing  $n_{eff}$  to realize a constant asymmetry of the molecular shape.

Table 3 compares structural parameters of DTDPE with those of PEs with longer unsaturated acyl chains (dioleoyl-PE, DOPE) and with shorter saturated alkyl chains (didodecyl-PE, DDPE) at a similar degree of hydration. Note that under conditions of excess water the chain melting transition of DTDPE ( $\sim 4 \text{ °C}$ ) is shifted by  $\sim 20 \text{ K}$  when compared with that of DOPE ( $\sim -16 \text{ °C}$ ).<sup>49</sup> Therefore, it seems reasonable to compare both lipids at identical hydration but at temperatures which differ by about 20 K. To compare the apparent lengths of the hydrocarbon chains,  $L_{hc}$ , we relate this quantity to the length of the corresponding saturated chain in the all-trans conformation,  $L_{max}$ . This relative chain length,  $L_{hc}/L_{max}$ , is nearly a constant,  $\sim 0.59\text{--}0.63$ , for the lipids with

(45) Kozlov, M. M.; Leikin, S.; Rand, R. P. *Biophys. J.* **1994**, *67*, 1603.  
 (46) Tate, M. W.; Gruner, S. M. *Biochemistry* **1989**, *28*, 4245.  
 (47) Seddon, J. M.; Ceys, G.; Marsh, D. *Biochemistry* **1983**, *22*, 1280.  
 (48) Lewis, R. N. A. H.; Mannock, D. A.; McElhaney, R. N.; Turner, D. C.; Gruner, S. M. *Biochemistry* **1989**, *28*, 541.  
 (49) Cullis, P. R.; de Kruijff, B. *Biochim. Biophys. Acta* **1978**, *513*, 31.

**Table 3. Comparison of Structural Parameters of DTDPE (45 °C), DDPE (135 °C),<sup>a</sup> and DOPE (22 °C)<sup>a</sup> at Identical Hydration Corresponding to  $r_w = 0.58$  nm**

	DOPE <sup>a</sup>	DDPE <sup>a</sup>	DTDPE	error
$n_{\text{eff}}$	18	12	14	
$A_{\text{pol}}$ , nm <sup>2</sup>	0.58	0.64	0.63	±0.02
$A_{\text{CB}}$ , nm <sup>2</sup>	1.13	1.06	1.11	±0.03
$L_{\text{hc}}$ , nm	1.27	0.91	1.04	±0.03
$L_{\text{hc}}/L_{\text{max}}^b$	0.62	0.59	0.63	±0.02
$D$ , nm	0.19	0.10	0.13	±0.03
$f_{\text{hc}}$	0.50	0.48	0.48	±0.03
$p_{\text{hc}} \propto f_{\text{hc}}/L_{\text{hc}}$ , nm <sup>-1</sup>	0.39	0.53	0.46	
$k_c$ , kJ·mol <sup>-1</sup> <sup>c</sup>	6	3	4	±0.8
$E_{\text{bend}}$ , kJ·mol <sup>-1</sup> <sup>c</sup>	1.5	1	1	±0.5

<sup>a</sup> Dimensions are calculated using the repeat distance given in refs 51 (DDPE) and 35 (DOPE). <sup>b</sup>  $L_{\text{max}}$  is the maximum length of the corresponding saturated hydrocarbon chain assuming the all-trans conformation:  $L_{\text{max}} = 1.65$  (DTDPE), 1.55 (DDPE), and 2.04 nm (DOPE). <sup>c</sup>  $k_c$  and  $E_{\text{bend}}$  are calculated according to eqs B3 and B5 using  $K_A = 0.2$  N/m.

different hydrocarbon chains (saturated, ether-linked; unsaturated, dienyl). Moreover, the area requirements per molecule at the polar/apolar interface,  $A_{\text{pol}}$ , and at the cell boundary,  $A_{\text{CB}}$ , are not very different for DTDPE, DOPE, and DDPE. Hence, the special property of the diene groups to promote the formation of the  $H_{\text{II}}$  phase is obviously not correlated to a special quality of the dimensions of the molecular aggregates.

When DOPE, DDPE, and DTDPE are compared at a constant degree of hydration, it turns out that the fraction of the lateral pressure that is caused by the hydrocarbon chains,  $f_{\text{hc}}$ , does not significantly depend on the thickness of the hydrophobic region and/or on the type of hydrocarbon chains (see Table 3). As a consequence, the offset distance,  $D$ , and thus also the bending moment,  $M$ , increase nearly linearly with  $L_{\text{hc}}$  (and  $n_{\text{eff}}$ , cf. eqs B2 and 10). On the other hand, the lateral pressure within the hydrophobic region,  $\pi_{\text{hc}}$ , is expected to depend linearly on the number of chain segments, i.e.,  $\pi_{\text{hc}} \propto n_{\text{eff}}$ .<sup>40,41</sup> For comparison of the lipids with different tails, it appears therefore convenient to normalize  $f_{\text{hc}} \propto \pi_{\text{hc}}$  (eq B1) to  $L_{\text{hc}} \propto n_{\text{eff}}$ , the effective thickness of the hydrophobic region across which  $\pi_{\text{hc}}$  acts. The normalization yields the amplitude of the (constant) pressure profile assumed, i.e.,  $p_{\text{hc}} = \pi_{\text{hc}}/L_{\text{hc}} \propto f_{\text{hc}}/n_{\text{eff}}$ . The correspondent values indicate that  $p_{\text{hc}}$  is considerably bigger for the lipids with the shorter hydrocarbon chains DDPE and DTDPE (Table 3). In other words, at an identical level of hydration the methylene, methyl, or methyne segments of the shorter hydrocarbon chains should repel each other more strongly to form a  $H_{\text{II}}$  structure than the segments of the longer acyl chains of DOPE.

Two mechanisms can be thought to cause the increased amplitude of the lateral pressure in the region of the tetradecadienyl chains: (1) a high degree of conformational disorder and/or (2) the partial interdigitation of the diene groups of the lipids which residue in opposite monolayers of the membrane.

The temperature and the enthalpy of the chain melting transition of DTDPC and DTDPE agree fairly well with the corresponding transition data which are predicted for disaturated lipids with nine CH<sub>2</sub> segments.<sup>4</sup> Hence, the acyl chains of DTDPE can be suggested to exist in a conformation similar to that of the hydrocarbon tails of a di-C<sub>11</sub>-PE at identical conditions. The long axes of the terminal diene groups are oriented on the average along the fiber axes of the hydrocarbon chains,<sup>19</sup> and thus these moieties virtually prolong the polymethylene sections by ~40% of their length (~1.16 nm). We suggest that the

terminal diene groups shift the position where  $\pi_{\text{hc}}$  effectively acts ( $z \approx -L_{\text{hc}}/2$ ) away from the polar/apolar interface. In this way also, the distance of the offset position of the lateral pressure,  $D$ , shifts toward the membrane center (cf. eq B2) and the resulting bending torque,  $M$ , exceeds that within a monolayer of the corresponding di-C<sub>11</sub> lipid. Hence, the PE lipid with terminal diene groups seems to combine the "fluidity" of the methylene segments of a di-C<sub>11</sub> lipid with an effective chain length of  $n_{\text{eff}} = 14$ . Of course, the polymethylene part of the tetradecadienyl chain is expected to exist in a more disordered conformation than the acyl chains of the corresponding disaturated C<sub>14</sub> lipid at identical conditions. Therefore, the  $H_{\text{II}}$  phase of DTDPE appears at lower temperatures and/or higher RH when compared with, e.g., DMPE. Indeed, we found that the difference between the  $L_{\alpha}/H_{\text{II}}$  and the gel/ $L_{\alpha}$  phase transition temperatures of fully hydrated DTDPE,  $T_{\text{h}} - T_{\text{m}} \approx 45$  K, is anomalously small in comparison with that of DMPE possessing an effective chain length of  $n_{\text{eff}} = 14$  ( $T_{\text{h}} - T_{\text{m}} \approx 95$  K).<sup>4,48</sup>

One can suggest an additional or alternative mechanism, namely, the partial interdigitation of the terminal diene groups in the center of the hydrophobic region. This effect can be expected to cause an additional lateral pressure component within the hydrophobic core which would tend to realize the asymmetric molecular shape as illustrated schematically in part C of Figure 9. IR linear dichroism measurements show that the terminal diene groups align essentially parallel to each other in the center of the hydrophobic region of lipid membranes.<sup>19</sup> In this way the diene moieties seem to rigidify the ends of the tetradecadienyl chains. One can suggest that this effect facilitates the partial interdigitation of terminal groups of lipids from opposite monolayers. Note that the interdigitation of the highly flexible methyl end groups of disaturated lipids is usually impeded in fluid membranes by entropic forces.

#### 4. Summary and Conclusions

The type of the lipid headgroups represents the most important factor that determines the hydration of lipid assemblies. Membranes of lipids with PE and PC headgroups which are polymerized in the center of the hydrophobic core show virtually identical water binding characteristics as the corresponding bilayers of monomeric lipids. This result raises the prospect to develop biocompatible materials with enhanced stability, on the one hand, and with a polar/apolar interface similar to that of biomembranes, on the other.

The short-range hydration force acting between hydrated interfaces is not affected by lipid polymerization. Consequently, contributions to the interbilayer repulsion which are caused by the mobility of individual molecules and/or the elastic deformation of the bilayers are obviously negligible at distances of less than a few tenths of nanometers.

Polymerization modifies the lateral compressibility of lipid bilayers in a drastic way. The polymerized lamellae become essentially incompressible in the direction parallel to the membrane surface owing to intermolecular covalent bonds. The frequencies of the methylene stretching bands correlate linearly with the area per molecules within the membrane plane. Consequently, infrared spectroscopy in combination with the osmotic stress technique represents a convenient method to estimate lateral compressibility in a qualitative way.

Terminal diene groups promote the formation of inverse structures possibly because of two mechanisms: (1) These

moieties act like a lever which “amplifies” the disordering effect of the polymethylene section of the acyl chains. (2) The rigid diene groups immobilize the otherwise highly flexible ends of the acyl chains and thus facilitate their partial interdigitation. It would be an interesting topic to study the influence of other rigid moieties in the terminal position on the phase behavior of lipids to generalize this finding. Investigations on lipids with terminal diacetylene groups are now in progress.

**Acknowledgment.** We are grateful to Prof. G. Klose for initiating some aspects of this work. We thank Dr. A. Anikin for the synthesis of the diene lipids. This work was supported by the Deutsche Forschungsgemeinschaft under Grants SFB294/C7 and SFB294/C10.

## APPENDICES

**A. Lateral Pressure of Lipid Bilayers.** Following the treatment given in ref 50 let us assume a surface layer consisting of  $N_W$  sorbent (water) and  $N_L$  sorbate (lipid) molecules, which may be considered as a single phase having the general properties of a two-component mixture. The Gibbs–Duhem relation yields for equilibration at isothermal and isobaric conditions

$$0 = N_L d\mu_L + N_W d\mu_W \quad (\text{A1})$$

It is convenient to use the fully hydrated lipid as the reference state. Insertion of  $d\mu_{W,L} = d\Delta\mu_{W,L}$  ( $\Delta\mu_{W,L} = \mu_{W,L}(a_W) - \mu_{W,L}(1)$ ) into eq A1 and rearrangement gives

$$d\Delta\mu_L = -R_{W/L} d\Delta\mu_W \quad (\text{A2})$$

where  $R_{W/L} = N_W/N_L$  is the molar ratio water/lipid. Making use of the definitions  $\pi_S = \Delta\mu_L/A_L$ ,  $\Pi = \Delta\mu_W/v_W$  (cf. eq 4), and  $d_W = 2R_{W/L}v_W/A_L$  (cf. the caption of Figure 3), one obtains from eq A2

$$d\pi_S = 0.5 d_W d\Pi \quad (\text{A3})$$

$\pi_S$  is the so-called two-dimensional spreading pressure.<sup>50</sup> In the present context,  $\pi_S$  is the difference in surface tension between the fully hydrated, “relaxed” surface and the partially dehydrated surface under osmotic stress.

Considering the empirical decay law of the hydration pressure,  $\Pi = \Pi_0 \exp(-d_W/\lambda)$  (cf. Table 2), one obtains from eq A3  $d\pi_S = -(\Pi_0/2\lambda) \exp(-d_W/\lambda) d_W d(d_W)$ . Integration yields

$$\pi_S = -\frac{\Pi_0}{2\lambda} \int_{\infty}^{d_W} d_W' \exp\left(-\frac{d_W'}{\lambda}\right) d(d_W') = \frac{1}{2}(d_W + \lambda)\Pi \quad (\text{A4})$$

(50) Ruthven, D. M. *Principles of Adsorption and Adsorption Processes*; John Wiley and Sons: New York, 1984.

(51) Seddon, J. M.; Cevc, G.; Kaye, R. D.; Marsh, D. *Biochemistry* **1984**, *23*, 2634.

(52) Scherer, J. R. *Biophys. J.* **1989**, *55*, 965.

The spreading pressure is just the increment of the lateral surface pressure which acts on a lipid monolayer upon dehydration. Let us assume two decoupled monolayers. Then one obtains for the bilayer

$$\Delta\pi_B = (d_W + \lambda)\Pi \quad (\text{A5})$$

**B. Components of the Lateral Pressure and the Bending Moment of the Monolayers in Lamellar and Hexagonal Phases.** Let us consider a lateral stress profile of a lipid monolayer according to the conditions  $p(z) = \pi_{\text{pol}}/L_{\text{pol}} = \text{constant}$  at  $0 < z < L_{\text{pol}}$ ,  $p(z) = \pi_{\text{hc}}/L_{\text{hc}} = \text{constant}$  at  $0 > z > -L_{\text{hc}}$ , and  $p(z) = 0$  otherwise (see Figure 9, part B for illustration). Integration of eqs 8 and 9 and rearrangement yield the fraction of the internal lateral pressure that is contributed by the lipid chains<sup>44</sup>

$$f_{\text{hc}} \equiv \frac{\pi_{\text{hc}}}{\pi_{\text{hc}} + \pi_{\text{pol}}} = \frac{L_{\text{pol}} + 2D}{L_{\text{hc}} + L_{\text{pol}}} \quad (\text{B1})$$

as a function of the offset position of the balanced forces,  $D$ , or alternatively

$$D = -\frac{1}{2}(f_{\text{hc}}(L_{\text{hc}} + L_{\text{pol}}) - L_{\text{pol}}) \quad (\text{B2})$$

as a function of  $f_{\text{hc}}$ . For the constant-pressure profile suggested,  $\pi_{\text{pol}}$  and  $\pi_{\text{hc}}$  effectively act at distances  $L_{\text{hc}}/2$  and  $L_{\text{pol}}/2$  from the polar/apolar interface, respectively. Following Marsh,<sup>44</sup> the bending moment,  $M = -\gamma D$ , is related to the intrinsic radius of curvature,  $R_0$ , and the curvature elastic constant,  $k_c$ , by  $M = -k_c/R_0$ .  $k_c$  can be expressed by

$$k_c = \frac{1}{4}N_A K_A R_0 D \quad (\text{B3})$$

where the offset distance of the internal lateral pressure is

$$D = \frac{1}{6R_0}(L_{\text{pol}}^2 + L_{\text{hc}}^2 - L_{\text{pol}}L_{\text{hc}}) \quad (\text{B4})$$

$K_A$  denotes the elastic constant for area extension/dilatation of a bilayer, i.e., of two monolayers (cf. eq 7). The intrinsic spontaneous radius of curvature of the monolayer,  $R_0$ , is assumed to be close to the radius of the polar cylinders in the inverse hexagonal phase, i.e.,  $R_0 \approx r_{\text{pol}}$ . The curvature elastic constant,  $k_c$ , scales the elastic curvature energy (per mole lipid)

$$E_{\text{bend}} = k_c A_{\text{pol}}/(2R_0^2) \quad (\text{B5})$$

which is necessary to “unbend” the monolayer to flatness (see ref 44 for details).

LA9900526